

Elastoplastic Micromechanical Analysis of FiberReinforced Composites with Defects

*Original*

Elastoplastic Micromechanical Analysis of FiberReinforced Composites with Defects / Nagaraj, M. H.; Kaleel, I.; Carrera, E.; Petrolo, M.. - In: AEROTECNICA MISSILI & SPAZIO. - ISSN 2524-6968. - ELETTRONICO. - 101:1(2022), pp. 53-59. [10.1007/s42496-021-00103-4]

*Availability:*

This version is available at: 11583/2959982 since: 2022-03-30T08:16:51Z

*Publisher:*

Aldo Frediani/Springer

*Published*

DOI:10.1007/s42496-021-00103-4

*Terms of use:*

This article is made available under terms and conditions as specified in the corresponding bibliographic description in the repository

*Publisher copyright*

Springer postprint/Author's Accepted Manuscript

This version of the article has been accepted for publication, after peer review (when applicable) and is subject to Springer Nature's AM terms of use, but is not the Version of Record and does not reflect post-acceptance improvements, or any corrections. The Version of Record is available online at: <http://dx.doi.org/10.1007/s42496-021-00103-4>

(Article begins on next page)

# Elastoplastic micromechanical analysis of fiber-reinforced composites with defects

M.H. Nagaraj · I. Kaleel · E. Carrera ·  
M. Petrolo

Received: date / Accepted: date

**Abstract** The objective of the present work is the computational micromechanical analysis of unidirectional fiber-reinforced composites, considering defects. The micromechanical model uses refined beam theories based on the Carrera Unified Formulation (CUF) and involves using the Component-Wise (CW) approach, resulting in a high-fidelity model. Defects are introduced in the representative volume element (RVE) in the form of matrix voids by modifying the material properties of a certain quantity of the Gauss points associated with the matrix. The quantity of Gauss points thus modified is based on the required void volume fraction, and the resulting set is prescribed a material property with negligible stiffness to model voids. Two types of void distribution are considered in the current work – randomly distributed voids within the matrix, and voids clustered in a region of the RVE. The current study investigates the influence of the volume fraction of voids present in the matrix and their distribution throughout the RVE domain on the macroscale mechanical response. Material nonlinearity is considered for the matrix phase. Numerical assessments are performed to investigate the influence of the volume fraction and the distribution of the voids on the macroscopic response.

**Keywords** Micromechanics · Defect modelling · High-Order Theories · CUF

---

M.H. Nagaraj  
Department of Mechanical Engineering, University of Massachusetts Lowell  
E-mail: Manish\_Nagaraj@uml.edu

I. Kaleel  
Deutsches Zentrum für Luft- und Raumfahrt e.V. (DLR), Institut für Test und Simulation  
für Gasturbinen, Virtuelle Turbine und numerische Methoden (VTM)

E. Carrera, M. Petrolo  
MUL2 Group, Department of Mechanical and Aerospace Engineering, Politecnico di Torino

## 1 Introduction

Fiber-reinforced composites are a popular engineering material in the aerospace and automobile industry owing to their high specific strength and stiffness. However, manufacturing limitations lead to various kinds of imperfections, especially in the microstructure, such as fiber misalignment and matrix voids. Such defects can have significant influences on the global mechanical properties of the structure. The proper characterization of voids and defects in the microstructure is therefore an important issue in the analysis of composite structures. A very common microstructural defect is the presence of voids in the matrix, which are formed due to trapped air during the curing of the composite. Voids have a significant influence on matrix-dominated mechanical properties such as compressive and interlaminar shear strength [1], and cause localization of stresses, thus acting as sites for failure initiation. From an experimental viewpoint, ultrasonic attenuation is an effective non-destructive approach to analyze such microstructural defects, since voids scatter elastic waves [2]. Various experimental studies involved the determination of the void morphology within the microstructure, both for unidirectional [3] and woven [4] composites. The influence of microstructural defects on mechanical properties has been studied by various researchers using computational mechanics. Such numerical approaches typically employ the finite element method due to its wide applicability. For instance, finite element analysis (FEA) was used to study the effects of void geometry on the elastic properties of unidirectional fiber-reinforced composites [5]. The effect of voids on the mechanical properties of 3D-woven carbon/carbon composites was investigated in [6, 7]. The effect of matrix defects on the interlaminar tensile fatigue behavior of carbon/epoxy composites was investigated in [8], and on the transverse mechanical properties of unidirectional composites in [9]. The aim of the present work is to investigate the effect of microstructural voids on the macroscale mechanical response of unidirectional fiber-reinforced composites. The analysis is based on the Carrera Unified Formulation (CUF), where expansion functions are employed to enhance the cross-sectional kinematics of 1D finite elements [10]. In particular, the current work uses the Component-Wise approach, where Lagrange polynomials are used as expansion functions thus leading to the explicit modeling of the various constituents in the microstructure. The use of such higher-order structural theories leads to an accurate evaluation of the 3D stress state, while avoiding the computational costs associated with 3D-FEA. Previous works on the topic of micromechanical analysis include the development of a micromechanics framework [11, 12] and its application to the progressive failure analysis of fibre-reinforced composites [13]. These works demonstrated the computational efficiency of the CUF micromechanics framework compared to standard 3D-FEA approaches, and the present work extends the previous work by modeling a more realistic microstructure of unidirectional fiber-reinforced composites, by considering matrix defects such as voids. The paper is arranged as follows – Section 2 introduces CUF, while Section 3 describes the microme-

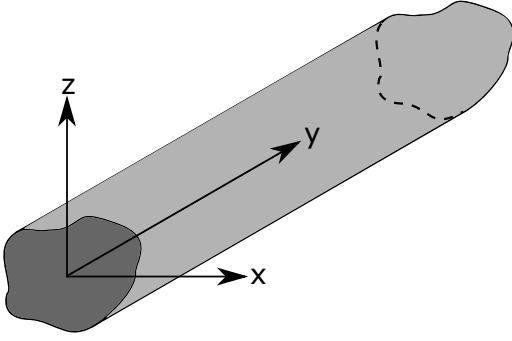


**Fig. 1** Arbitrary beam element in CUF coordinate system

chanics framework. Some numerical assessments are presented in Section 4, followed by the conclusions in Section 5.

## 2 1D structural theories

### 2.1 Carrera unified formulation

Consider a beam element as shown in Fig. 1. The generalized displacement field is given by

$$\mathbf{u} = F_\tau(x, z)\mathbf{u}_\tau(y), \tau = 1, 2, \dots, M \quad (1)$$

Where  $\mathbf{u}$  is the displacement field and  $F_\tau(x, z)$  is the expansion function across the cross-section.  $\mathbf{u}_\tau$  is the generalized displacement vector, and  $M$  is the number of terms in the expansion function. The choice of  $F_\tau$  and  $M$  is arbitrary. The present work considers the Component-Wise (CW) approach, which exploits Lagrange polynomials to enhance the cross-section kinematic field of 1D finite elements. Additionally, this approach leads to purely displacement degrees of freedom in the system. As an example, the displacement field obtained by a quadratic Lagrange polynomial is

$$\begin{aligned} u_x &= \sum_{\tau=1}^9 F_\tau(x, z) \cdot u_{x_\tau}(y) \\ u_y &= \sum_{\tau=1}^9 F_\tau(x, z) \cdot u_{y_\tau}(y) \\ u_z &= \sum_{\tau=1}^9 F_\tau(x, z) \cdot u_{z_\tau}(y) \end{aligned} \quad (2)$$

Further details on the use of Lagrange polynomials as a class of expansion functions can be found in [14].

## 2.2 Finite element formulation

The stress and strain fields are given by

$$\begin{aligned}\boldsymbol{\sigma} &= \{\sigma_{xx} \ \sigma_{yy} \ \sigma_{zz} \ \sigma_{xz} \ \sigma_{yz} \ \sigma_{xy}\}^T \\ \boldsymbol{\epsilon} &= \{\varepsilon_{xx} \ \varepsilon_{yy} \ \varepsilon_{zz} \ \varepsilon_{xz} \ \varepsilon_{yz} \ \varepsilon_{xy}\}^T\end{aligned}\quad (3)$$

Considering linear strains, the strain-displacement relation is given by

$$\boldsymbol{\epsilon} = \mathbf{D}\mathbf{u} \quad (4)$$

where  $\mathbf{D}$  is the linear differentiation operator. The constitutive law makes use of the elastoplastic stress-strain relation,

$$\boldsymbol{\sigma} = \mathbf{C}^{cep} \boldsymbol{\epsilon} \quad (5)$$

where  $\mathbf{C}^{cep}$  stands for the consistent elastoplastic tangent material matrix. The present work models matrix nonlinearities using the von Mises plasticity model. The structure is modeled using 1D finite elements with standard shape functions  $N_i(y)$ , and the resulting displacement field is written as

$$\mathbf{u}(x, y, z) = F_\tau(x, z) N_i(y) \mathbf{u}_{\tau i} \quad (6)$$

where  $\mathbf{u}_{\tau i}$  is the nodal displacement field. For the quasi-static nonlinear problem, the principle of virtual work is herein recalled,

$$\delta L_{\text{int}} = \delta L_{\text{ext}} \quad (7)$$

where  $\delta L_{\text{int}}$  is the virtual variation of the strain energy and  $\delta L_{\text{ext}}$  is the virtual variation of the work of the external loads. The virtual variation of the internal work can be expressed as:

$$\delta L_{\text{int}} = \int_V \delta \boldsymbol{\epsilon}^T \boldsymbol{\sigma} \, dV \quad (8)$$

where  $V$  is the volume of the body. Introducing the constitutive relations,

$$\delta L_{\text{int}} = \delta \mathbf{u}_{sj}^T \left( \int_V \mathbf{D}_{sj}^T \mathbf{C}^{cep} \mathbf{D}_{\tau i} \, dV \right) \mathbf{u}_{\tau i} \quad (9)$$

Looping through the four indices  $i, j, \tau, s$  results in the element stiffness matrix, which is then assembled to generate the global stiffness matrix.

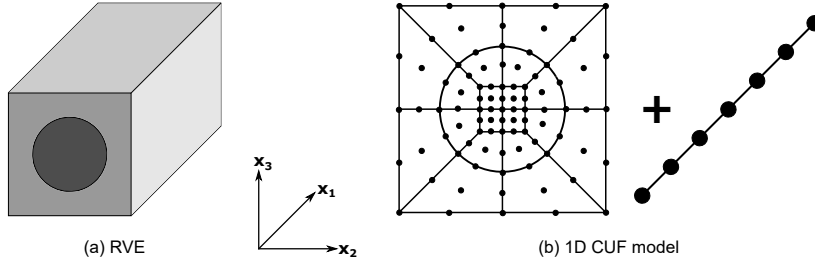


**Fig. 2** Component-Wise modelling of the RVE using 1D CUF

### 3 Micromechanical analysis

Considering the CW approach, the representative volume element (RVE) is modeled using 1D-CUF theories, where the beam models the RVE depth and Lagrange elements model the cross-section, i.e., the  $x_2$ - $x_3$  plane, as shown in Fig. 2. The micromechanics framework is based on the periodic nature of the RVE, and periodic boundary conditions (PBC) are applied to ensure displacement compatibility across the faces of the RVE [15]. The displacements applied on opposite RVE surface pairs is given by

$$u_i^{j+}(x, y, z) - u_i^{j-}(x, y, z) = \bar{\epsilon}_{ik}(x_k^{j+} - x_k^{j-}) \quad (10)$$

where  $\bar{\epsilon}_{ik}$  is the applied macroscopic strain, indices  $j+$  and  $j-$  represent the positive and negative directions, respectively, along  $x_k$ . The homogenized stress ( $\bar{\sigma}_{ij}$ ) and strain ( $\bar{\epsilon}_{ij}$ ) response is obtained by volume averaging the microscopic fields ( $\sigma_{ij}$ ,  $\epsilon_{ij}$ ) [16],

$$\bar{\epsilon}_{ij} = \frac{1}{V} \int_V \epsilon_{ij} dV \quad (11)$$

$$\bar{\sigma}_{ij} = \frac{1}{V} \int_V \sigma_{ij} dV \quad (12)$$

where  $V$  is the RVE volume. The constitutive relation for the homogenized medium reads as

$$\bar{\sigma}_{ij} = \bar{C}_{ijkl} \bar{\epsilon}_{kl} \quad (13)$$

where  $\bar{C}_{ijkl}$  is the homogenized material matrix. A detailed explanation of the 1D micromechanics framework in CUF is given in [11].

Matrix voids within the RVE are modelled by selecting a certain quantity of Gauss points associated with the matrix constituent and assigning a material property to them with negligible stiffness. The number of such Gauss points depends on the required void volume fraction specified by the user. The distribution of the voids can also be specified by controlling the selection procedure of the matrix Gauss point set. Further details on the modelling of matrix voids within the RVE may be found in [12]. Two types of void distribution are considered in the current work – randomly distributed voids within the matrix, and voids clustered in a region of the RVE. The current study investigates the influence of the volume fraction of voids present in the matrix,

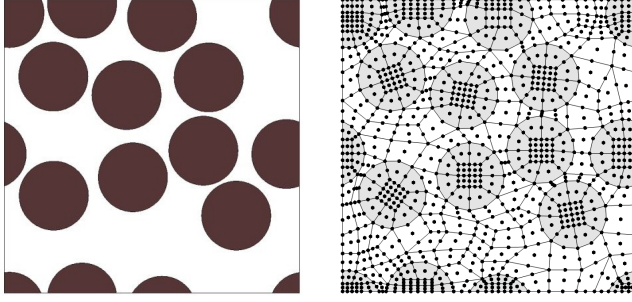


**Fig. 3** Schematic diagram of the RVE with randomly distributed fibres (left), and the L9 cross-sectional discretisation (right)

**Table 1** Properties of the constituent materials, the units of the elastic moduli are GPa

Material	$E_{11}$	$E_{22}=E_{33}$	$G_{12}=G_{13}=G_{23}$	$\nu_{12}=\nu_{13}$	$\nu_{23}$
Fiber	276	16	5	0.28	0.31
Matrix	3.5	3.5	1.3	0.35	0.35

as well as their distribution throughout the RVE domain, on the macroscale mechanical response.

## 4 Numerical results

### 4.1 Micromechanical analysis of RVE without defects

The first numerical assessment involves the micromechanical analysis of a pristine RVE, i.e. without defects. A randomly distributed RVE is considered with a fibre volume fraction  $V_f = 0.47$ . The 1D-CUF model consists of 2 four-node beam (B4) elements in the 11-direction to describe the RVE depth, and 277 nine-node bi-quadratic expansions (L9) to describe the cross-section. A schematic representation of the RVE architecture, as well as its discretization, is shown in Fig. 3. The fibre constituent is modelled as a linear-elastic material. Nonlinearity is introduced within the matrix constituent, modelled as an elastoplastic material based on the J2 plasticity theory. Further details on the implementation of this constitutive model within CUF is found in [17]. The constituent material properties are listed in Table 1 and the plasticity curve, which defines the nonlinear matrix behaviour, is plotted in Fig. 4. Two load cases have been considered in the current assessment, where strains are applied in the 22- and 23-direction of the RVE, respectively. The magnitude of applied strain in both cases is 0.02. The macroscopic stress-strain response for the loading cases is plotted in Fig. 5. Dehomogenization is also performed to obtain the local stress and strain fields within the RVE. The von Mises stress field (MPa) and equivalent plastic strain distribution for the case of 22-direction loading is shown in Fig. 6, while that for the case of 23-direction loading is shown in Fig. 7.

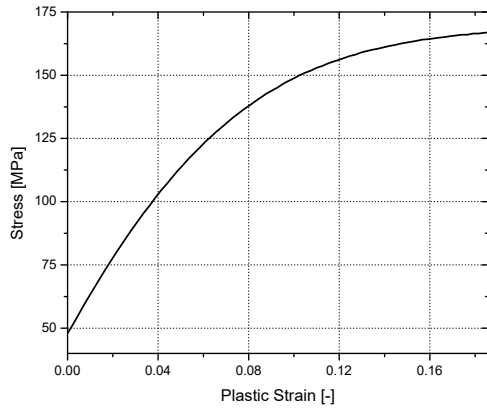


**Fig. 4** Stress – plastic strain curve of the elastoplastic matrix

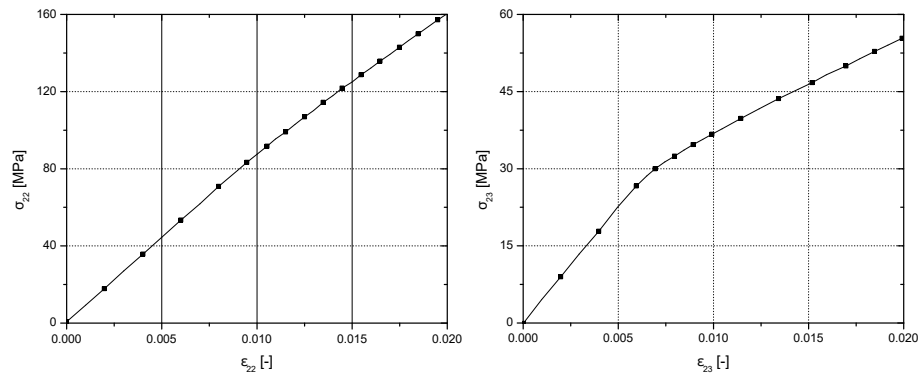


**Fig. 5** Macroscopic stress-strain response for the pristine RVE, for strains applied in the 22-direction (left) and the 23-direction (right), stress reported in MPa

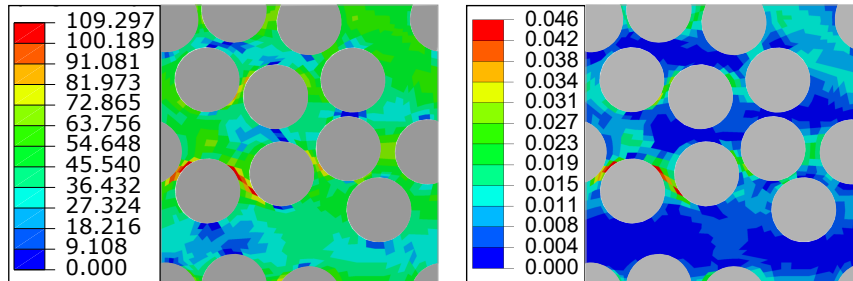


**Fig. 6** von Mises stress (MPa, left) and eq. plastic strain (right) for the pristine RVE loaded in the 22-direction



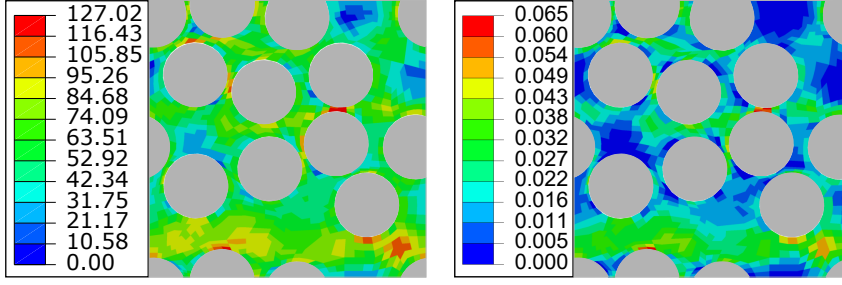


**Fig. 7** von Mises stress (MPa, left) and eq. plastic strain (right) for the pristine RVE loaded in the 23-direction

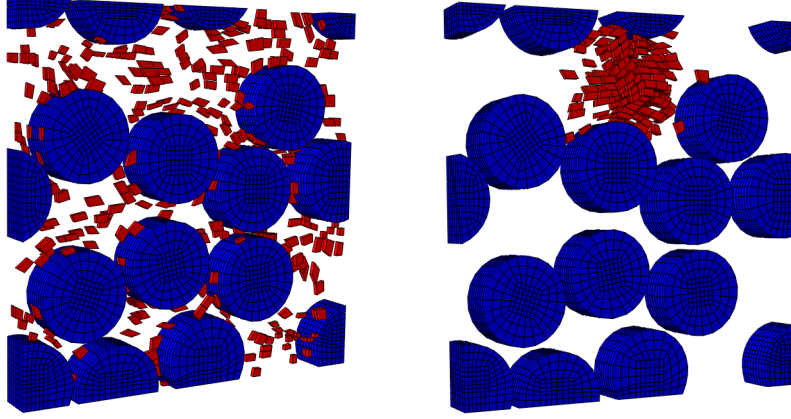


**Fig. 8** Schematic representation of the RVE with 2% voids in the matrix. Randomly distributed voids (left), and clustered voids (right)

#### 4.2 Micromechanical analysis of RVE with defects

The RVE shown in Fig. 3 is considered again, now with defects in the form of matrix voids. A void volume fraction of 2% has been used for the current assessment. Two versions of the RVE are analyzed, one with randomly distributed voids and the other with clustered voids, to investigate the effect of void distribution on the microscale fields. The two RVEs with different void distributions are schematically shown in Fig. 8. Dehomogenization analysis is carried out to determine the local stress and strain fields within the RVE. In this case, a strain is applied in the 22-direction. The distribution of the von Mises stress and equivalent plastic strains for the case of the randomly distributed voids is given in Fig. 9, while that for the case of clustered voids is shown in Fig. 10. The following observations are made:

- Stress concentration occurs in the vicinity of the voids, and the stress magnitude increases compared to the pristine RVE. This is seen by comparing the von Mises stress fields in Fig. 6 with those in Figs. 9 and 10.

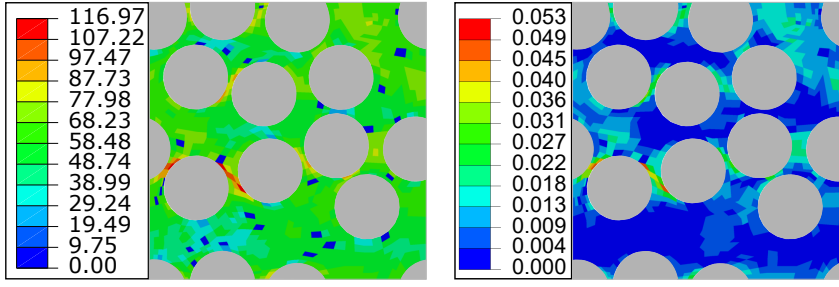


**Fig. 9** von Mises stress (MPa, left) and eq. plastic strain (right) for the RVE with randomly distributed voids

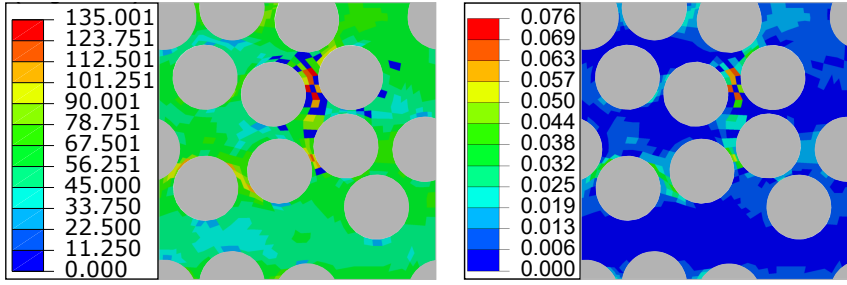


**Fig. 10** von Mises stress (MPa, left) and eq. plastic strain (right) for the RVE with clustered voids

- The increased magnitude of von Mises stresses leads to higher plasticity, as seen in Figs. 9 and 10.
- Clustered voids lead to higher stress concentration, and consequently plastic effects, compared to randomly distributed voids.

#### 4.3 Influence of the void fraction

The final numerical assessment is the investigation of the influence of the void fraction on the overall macroscopic stress-strain response. Various RVEs are developed with void fractions ranging from 1-4%, and both random and clustered void distributions are considered. A strain of magnitude 0.02 is applied in the 22-direction. Homogenisation is performed to determine the macroscale stress-strain response. The normalized macro-stress as a function of void fraction is plotted and the macroscopic stress-strain response for a void fraction of 4% are plotted in Fig. 11. The following comments are made:

- The computed macro-stress reduces as the void fraction is increased.
- The presence of voids leads to a reduction in the macroscale material stiffness, which can significantly influence global mechanical behavior.
- In all cases, clustered voids lead to a greater reduction in stresses compared to randomly distributed voids, owing to increased localization of plasticity.

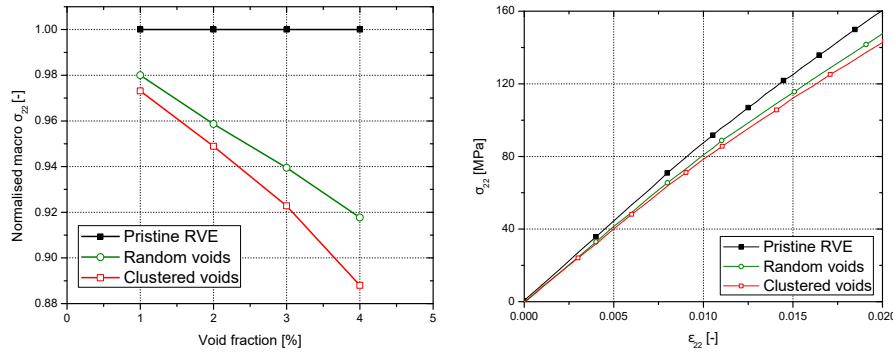


**Fig. 11** Influence of void fraction on macroscopic stress response (left), and macroscopic stress-strain response for a void fraction of 4% (right); stress in MPa

## 5 Conclusions

The present work investigated the effect of microstructural matrix voids on the macroscale mechanical behavior of unidirectional fiber-reinforced composites. The analysis was performed via a micromechanics framework based on refined beam theories, obtained using the Carrera Unified Formulation. Periodic boundary conditions were used to maintain consistency with the repeating nature of the RVE. Homogenization was performed to obtain the macroscopic response, while dehomogenization provided the local stress and strain fields. The influence of voids on the global mechanical behavior was studied, both in terms of the void volume fraction, as well as void distribution through the RVE. It was shown that the increase of voids leads to significant reductions in the macroscale stiffness of the composite. It was also observed that clustered voids are more critical than randomly distributed voids, since a clustered configuration develops higher stress concentration, leading to more localized plasticity, eventually resulting in significant reduction of the structural mechanical performance. Future works include micromechanical progressive damage analysis, considering voids, as well as structural analysis based on multiscale approaches.

## Conflict of interest statement

On behalf of all authors, the corresponding author states that there is no conflict of interest.

## References

1. H. Jeong. Effects of voids on the mechanical strength and ultrasonic attenuation of laminated composites. *Journal of composite materials*, 31(3):276–292, 1997.
2. R. Prakash. Non-destructive testing of composites. *Composites*, 11(4):217–224, 1980.

3. D.E.W. Stone and B. Clarke. Ultrasonic attenuation as a measure of void content in carbon-fibre reinforced plastics. *Non-destructive testing*, 8(3):137–145, 1975.
4. D.K. Hsu. Ultrasonic measurements of porosity in woven graphite polyimide composites. In Springer, editor, *Review of Progress in Quantitative Nondestructive Evaluation*, pages 1063–1068. 1988.
5. H. Huang and R. Talreja. Effects of void geometry on elastic properties of unidirectional fiber reinforced composites. *Composites Science and Technology*, 65(13):1964–1981, 2005.
6. M.V. Rao, P. Mahajan, and R.K. Mittal. Effect of architecture on mechanical properties of carbon/carbon composites. *Composite Structures*, 83(2):131–142, 2008.
7. A. Shigang, F. Daining, H. Rujie, and P. Yongmao. Effect of manufacturing defects on mechanical properties and failure features of 3D orthogonal woven C/C composites. *Composites Part B: Engineering*, 71:113–121, 2015.
8. G. Seon, A. Makeev, Y. Nikishkov, and E. Lee. Effects of defects on interlaminar tensile fatigue behavior of carbon/epoxy composites. *Composites Science and Technology*, 89:194–201, 2013.
9. D.A. Vajari, C. González, J. Llorca, and B.N. Legarth. A numerical study of the influence of microvoids in the transverse mechanical response of unidirectional composites. *Composites Science and Technology*, 97:46–54, 2014.
10. E. Carrera, M. Cinefra, M. Petrolo, and E. Zappino. *Finite element analysis of structures through unified formulation*. John Wiley & Sons, 2014.
11. I. Kaleel, M. Petrolo, A.M. Waas, and E. Carrera. Computationally efficient, high-fidelity micromechanics framework using refined 1D models. *Composite Structures*, 181:358–367, 2017.
12. E. Carrera, M. Petrolo, M.H. Nagaraj, and M. Delicata. Evaluation of the influence of voids on 3D representative volume elements of fiber-reinforced polymer composites using CUF micromechanics. *Composites Structures*, 254, 2020.
13. I. Kaleel, M. Petrolo, A.M. Waas, and E. Carrera. Micromechanical progressive failure analysis of fiber-reinforced composite using refined beam models. *Journal of Applied Mechanics*, 85(2), 2018.
14. E. Carrera and M. Petrolo. Refined beam elements with only displacement variables and plate/shell capabilities. *Meccanica*, 47(3):537–556, 2012.
15. Z. Xia, Y. Zhang, and F. Ellyin. A unified periodical boundary conditions for representative volume elements of composites and applications. *International Journal of Solids and Structures*, 40(8):1907–1921, 2003.
16. C.T. Sun and R.S. Vaidya. Prediction of composite properties from a representative volume element. *Composites Science and Technology*, 56(2):171–179, 1996.
17. E. Carrera, I. Kaleel, and M. Petrolo. Elastoplastic analysis of compact and thin-walled structures using classical and refined beam finite element models. *Mechanics of Advanced Materials and Structures*, 26(3):274–286, 2019.